Vol. 55: 167–179, 2012
doi: 10.3354/cr01132

CLIMATE RESEARCH
Clim Res

Published online December 13

High-resolution precipitation over the southern Balkans

C. J. Lolis*

Laboratory of Meteorology, Department of Physics, University of Ioannina, 45110 Ioannina, Greece

ABSTRACT: The main climatic characteristics of precipitation in the southern Balkans were examined by applying S-Mode and T-Mode factor analysis (FA) to APHRODITE 0.25° × 0.25° grid point precipitation data for the period 1951–2007. First, S-Mode FA was applied to the seasonal precipitation values and revealed the main modes of interannual variation of precipitation for each season. These modes were found to be connected to specific atmospheric circulation centers of action. Statistically significant negative trends were found for: (1) winter and spring precipitation over northwestern Greece and southern Albania and (2) spring and autumn precipitation over the southern Aegean Sea. Next, T-Mode FA was applied to the 57 yr mean precipitation of 5 d intervals (n = 73) in a year and resulted in 3 main modes of spatial distribution of precipitation: (1) the cold period mode (late November to late March) with maxima in northwestern Greece and the western Asia Minor coasts, (2) the warm period mode (late April to late August), presenting a maximum over the northern continental areas, and (3) the autumn mode (early September to late October) with a maximum found over the northern Ionian Sea. The intra-annual variations of the prevalence degree of these modes are connected to the seasonality of the thermal characteristics of the surface and the overlying atmospheric layers and the main circulation systems affecting the region.

KEY WORDS: Precipitation variability · Southern Balkans · Mediterranean Sea

1. INTRODUCTION

The Balkan Peninsula is an area of southeastern Europe located in a climatologically sensitive zone between the subtropics and the temperate latitudes. It experiences a strong seasonal cycle involving most of the climatic parameters associated with the seasonality of the main large-scale circulation systems affecting the region (e.g. Lolis et al. 2008). Precipitation in the southern Balkans has an uneven spatial distribution because of the complex geomorphological characteristics of the region. The presence of the Pindus and Rodopi mountain ranges, the variant topography and abrupt elevation changes, the many plateaus and valleys, and the extensive and complex coastline ensure that the local orographic effects and the orientation of the various regions are dominant factors for precipitation formation. Sometimes, the contribution of the above factors to precipitation formation becomes more significant than that of the synoptic-scale systems. Therefore, the examination of the climatic characteristics of precipitation in this region reveals its meteorological particularities. The basic climatic characteristics of precipitation in the southern Balkans have been examined by numerous researchers, mainly on a monthly basis (see e.g. Kotini-Zabaka 1983, Fotiadi et al. 1999, Metaxas et al. 1999, Xoplaki et al. 2000, Bartzokas et al. 2003a,b, Hatzianastassiou et al. 2008, Türkeş et al. 2009, Kambezidis et al. 2010, Unal et al. 2012).

The intra-annual precipitation variability is strongly influenced by the seasonality of (1) the lower troposphere vertical stability modulated by the thermal characteristics of the land and sea surfaces and the overlying atmospheric layers and (2) the strength and the position of the large-scale synoptic systems

*Email: chlolis@cc.uoi.gr

affecting the region. Such systems encompass the Azores subtropical anticyclone and the SW Asia thermal low (see e.g. Metaxas & Bartzokas 1994, Davis et al. 1997). During summer, the subtropical anticyclone contributes to the advection of warm and dry air masses of subtropical origin over the Mediterranean. This advection combined with the high static stability over the cool (relatively to the air above it) Mediterranean Sea surface leads to dry and sunny weather, especially over marine and coastal areas. In contrast, during winter, the SW Asia thermal low is not a prominent feature, and the Azores subtropical anticyclone is weakened and southward-displaced. The presence of the southward displaced jet stream, the high baroclinicity along the northern Mediterranean coasts, and the influence of the neighboring mountain ranges (e.g. the Alps) on the westerly air flow lead to the formation of the typical Mediterranean depressions, mainly over the Gulfs of Lion and Genoa (see e.g. Alpert et al. 1996, Maheras et al. 2001, Trigo et al. 2002). These depressions propagate eastwards along the Mediterranean Sea, being enhanced due to the upward sensible and latent heat fluxes. The aforementioned combined with the high static instability over the warm (relative to the overlying air) sea surface lead to high precipitation in the Greek peninsula and the adjacent seas, especially over the western windward flanks, where convective instability is also a dominant factor for precipitation formation (e.g. Lolis et al. 2004). The seasonal variation in the above factors has a relatively low fine-scale variation, and this would normally lead to a similarly 'smooth' intra-annual variation in precipitation. However, secondary maxima and minima are also found in this intra-annual variation. These secondary fluctuations are of an order lower than 1 mo and cannot be revealed using monthly data. Analyses based on 10 or 5 d precipitation values are appropriate for such an examination (e.g. Bartzokas et al. 2003a).

The interannual variability of precipitation in the southern Balkans is significantly affected by the North Atlantic Oscillation (NAO), which modifies the main depression trajectories over the region under study (e.g. Hurrel & van Loon 1997, Trigo 2006, Chronis et al. 2011). A positive NAO phase (high NAO index) is associated with lower than normal values of precipitation in the southern Balkans, as it is responsible for a northward displacement of the jet stream and the corresponding depression trajectories. In contrast, a negative NAO phase (low NAO index) is associated with higher depression activity in the Mediterranean and higher than normal precipitation in the southern Balkans (Hatzianastassiou et al. 2008, Nastos 2011, Philandras et al. 2011). Furthermore, the Saharan depressions, formed along the Atlas Mountains and moving towards the eastern Mediterranean, contribute significantly to precipitation in the southeastern areas of the Greek peninsula (e.g. Prezerakos et al. 1990, Thorncroft & Flocas 1997, Bartzokas et al. 2003b).

In the present study, the spatial and temporal variability of precipitation in the southern Balkans was examined by applying a multivariate statistical methodology to the APHRODITE (Asian Precipitation – Highly-Resolved Observational Data Integration Towards Evaluation of Water Resources) data set, which is a new high-resolution precipitation data set for Asia and the eastern Mediterranean (Yatagai et al. 2012). The basic advantage of using a gridded instead of non-gridded data set is the uniform spatial coverage, which leads to a spatially representative data input, suitable for a multivariate statistical analysis. The results of the present study may provide useful evidence regarding the characteristics of the relatively complicated precipitation climatology in the southern Balkans as well as regarding the validity of the data set over a region with such complex geomorphological characteristics. Furthermore, the detailed examination of precipitation climatology in a region located in the transitional area between temperate and subtropical climate zones may reveal significant trends associated with ongoing global climate change.

2. METHODS

Daily grid point data for the period 1951–2007 (57 yr) were used. The data consisted of:

(1) 0.25° × 0.25° precipitation values over the southern Balkans (19–29° E, 34–42° N; Fig. 1) obtained from the APHRODITE precipitation data base. The APHRODITE project develops state-of-the-art daily precipitation data sets with high-resolution grids. The data sets are created primarily with data obtained from a rain gauge observation network (Yatagai et al. 2012). The status of data collection and the domains used to create the daily grids are available at www.chikyu.ac.jp/precip/index.html. Some attempts have been made to compare of the APHRODITE data base with other gridded precipitation data sets such as GPCC and TRMM (e.g. Javanmard et al. 2010, Yatagai et al. 2012). In the present study, we used APHRO_MA_V1003R1, which has better quality control and incorporates more data when compared with APHRO_MA_V0902 (Yatagai et al. 2008, 2009; in

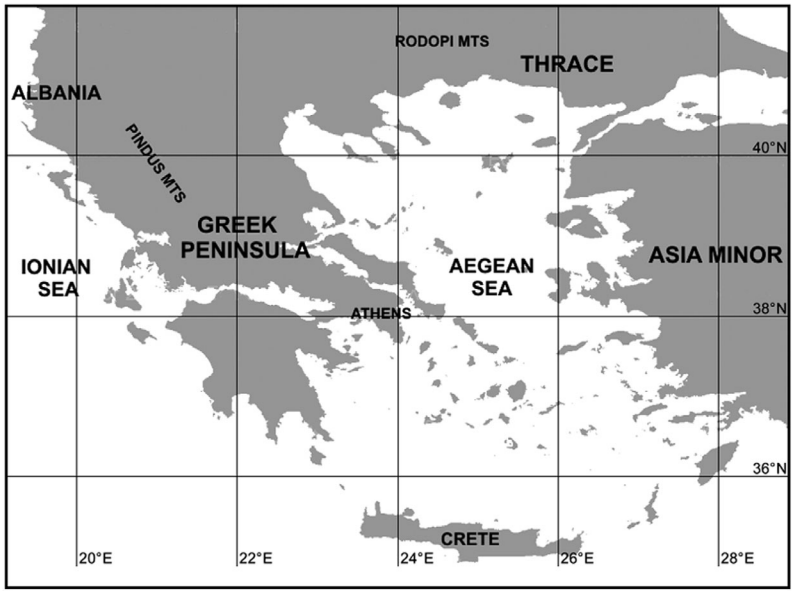

Fig. 1. Southern Balkans, showing the locations of the main geographical areas referred to in the text

addition, bugs in the software have been corrected). Of the 1280 points of the above grid, we used only 727, because the remaining points correspond to missing values.

(2) 2.5° × 2.5° 500 hPa geopotential height (GH) anomalies over Europe and the Mediterranean (20°W – 40°E, 25–60°N), obtained from the NCEP/NCAR Reanalysis data set (Kalnay et al. 1996, Kistler et al. 2001).

The winter, spring, and autumn precipitation values and the 57 yr mean values (mean values for the period 1951–2007) for 5 d intervals (n = 73) of the year (73 intervals × 5 d = 365 d) were calculated. The long-term mean 5 d values were used instead of the long-term mean daily or monthly values, because the 73 values provide a sufficient intra-annual analysis of precipitation (more detailed than using only the 12 monthly values), without taking into account the day-to-day variations, which (from a climatological point of view) are not important. The long-term mean day-to-day variations may considerably deviate from the climatological means, since >57 yr data are required for such a detailed approach (Lolis et al. 2008). Next, 4 matrices were constructed: 1 matrix (56 × 727) for winter (the period for winter is 1952–2007, 56 yr), 2 matrices (57 × 727) for the other 2 seasons (1 for spring and 1 for autumn), and 1 matrix (73 × 727) for the mean 5 d values. The lines of the matrices correspond to time (years or 5 d intervals) and the columns correspond to space (grid points).

Factor analysis (FA) is a dimensionality reduction statistical method that expresses a set of p correlated variables X_1, X_2, ..., X_p in terms of a smaller number of new uncorrelated indices, elucidating the relationship between the original p variables (Jolliffe 1986, Manly 1986). Each of the p initial variables is expressed as a linear function of m ($m < p$) factors, i.e. $Xi = a_{i1}F_1+a_{i2}F_2+...+a_{im}F_m$, where F_1, F_2, ..., F_m are the factors and a_{i1}, a_{i2}, ..., a_{im} are the respective loadings. The values of F_1, F_2, ..., F_m are called scores and are usually presented in standardized format. FA is a multivariate statistical method similar to principal component analysis (PCA) and empirical orthogonal functions, which are frequently used in climatology (e.g. García-Serrano et al. 2011, Tatli & Türkeş 2011). PCA and FA become essentially equivalent if the error terms in the FA model (the variability not explained by common factors) can be assumed to all have the same variance (e.g. Manly 1986). The number (m) of the retained factors is decided by using various rules (Overland & Preisendorfer 1982, Jolliffe 1986) and considering the physical interpretation of the results (e.g. Bartzokas & Metaxas 1993).

In the present study, a SCREE plot was taken into account as a general rule about the selection of m. According to this criterion, m equals the number of points deviating from a straight line in a plot of the correlation matrix eigenvalues, ordered from highest to lowest. There are various modes of FA. For example, the mode of FA is S when it is applied to a matrix characterized by lines and columns referring to time and space, respectively, while the mode of FA is T when it is applied to a matrix characterized by lines and columns referring to space and time, respectively (Richman 1986). In an S-mode FA, the spatial patterns of the loadings indicate the areas that correspond to the main components of the examined parameter, while the time series of the scores indicate the variation of this parameter in the above areas. In a T-mode FA, the spatial patterns of the scores show the dominant types of spatial distribution of the examined parameter, while the time series of the loadings indicate the variation of the predominance degree of these patterns. A widely used process is the rotation of the axes. Rotation succeeds in a better discrimination among the variables and thus in a better interpretation of the results. It overcomes certain characteristics of the unrotated solutions (e.g. dependence on the domain, subdomain stability, sam-

pling errors) that obscure the isolation of the individual modes of variation (Richman 1986). Here we used S-mode and T-mode FA with varimax rotation.

S-Mode FA was applied to the 57 × 727 and 56 × 727 matrices consisting of seasonal values in order to reveal the main modes of inter-annual variation of precipitation for each season. The analysis was not applied to summer, because during summer, precipitation over the area under study is rare especially over the sea, and its inter-annual variation is mainly modulated by isolated (in time and space) extreme events associated with thunderstorm activity, which cannot be treated on a seasonal basis. In order to obtain a physical interpretation of the factors found, the mean patterns of 500 hPa GH anomalies over Europe were constructed for the years that correspond to the 10% highest and 10% lowest scores of the factors, and the score time series were correlated to the large-scale teleconnection indices over the North Atlantic and Eurasia. The statistical significance (95% confidence level) of the linear trends found was tested using the Mann-Kendall statistical test. T-Mode FA was then applied to the 727 × 73 matrix (the transposition of the initial 73 × 727 matrix) consisting of mean 5 d values in order to reveal the main characteristic precipitation patterns and the intra-annual variation of their predominance degree. Thus, the basic characteristics of precipitation in the southern Balkans concerning the respective inter-annual variability and the intra-annual variation of the respective spatial distribution can be revealed.

3. RESULTS AND DISCUSSION

3.1. Inter-annual variability

For winter, Fig. 2a illustrates the spatial distribution of the long-term mean precipitation. Winter precipitation is highest in the north Ionian Sea and north-western Greece (west of the Pindus mountain range) and also in the east Aegean Sea and southwestern Asia Minor. In contrast, precipitation has lower values in the eastern leeward areas of the Greek peninsula and the central Aegean

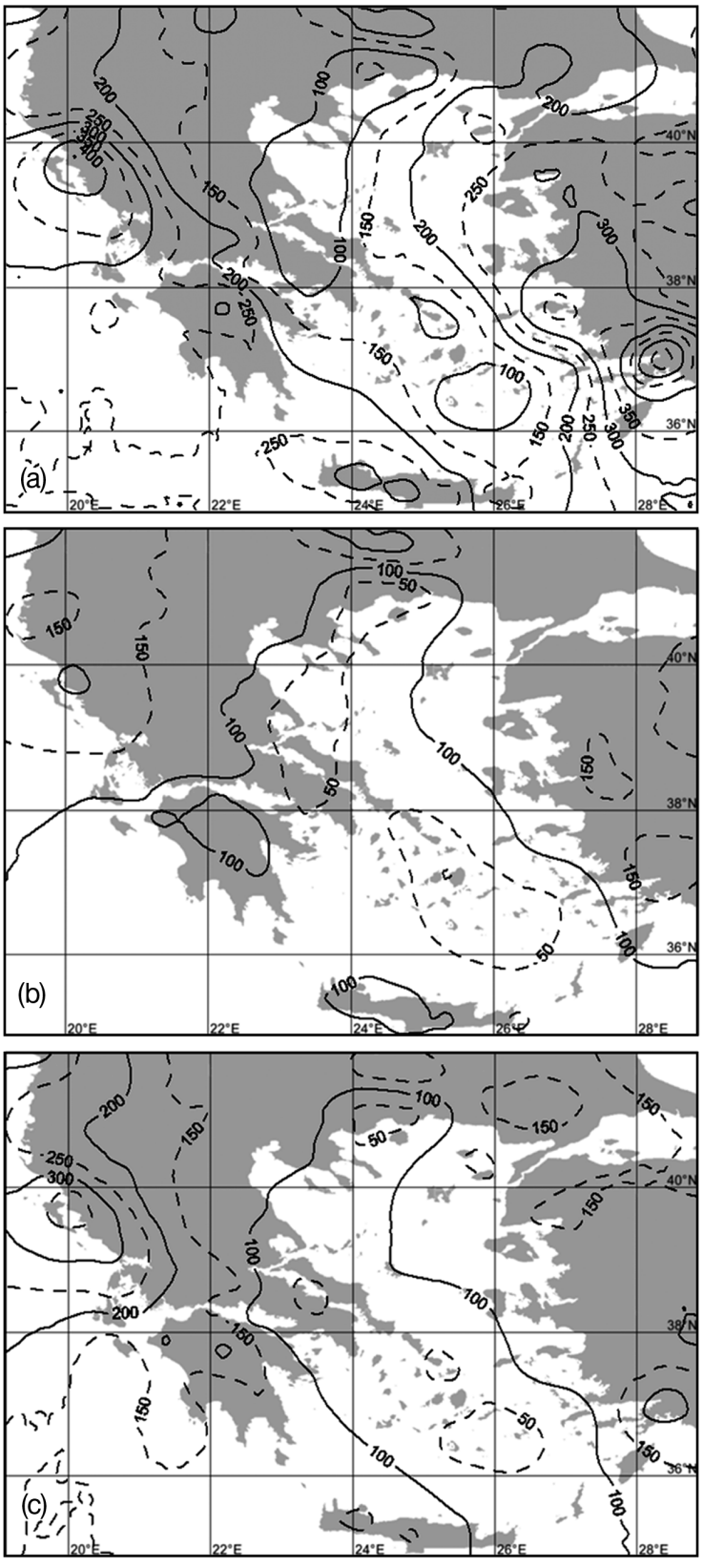

Fig. 2. Spatial distribution of mean precipitation height (mm) in the southern Balkans, for the period 1952–2007: (a) winter, (b) spring, (c) autumn

Sea. This spatial distribution is in agreement with the fact that during winter, the circulation over the eastern Mediterranean is mainly zonal. The depressions formed primarily over the Gulfs of Lion and Genoa are associated with a southwesterly flow being responsible for high precipitation in the western windward areas (e.g. Bartzokas et al. 2003a,b). The application of FA to winter leads to 4 factors accounting for 79% of the total variance. The isopleths of factor loadings are presented in Fig. 3a (isopleths for loadings ≥0.6 are shown), the inter-annual variations of factor scores are presented in Fig. 3b–e, and the mean 500 hPa GH anomaly patterns for the winters that correspond to the 6 (10%) highest and the 6 lowest scores of the factors are presented in Fig. S1a–h in the supplement (available at www.int-res.com/articles/suppl/c055p167_supp.pdf). Factor 1 represents the inter-annual variation of winter precipitation in northwestern Greece and southern Albania (Fig. 3a). It is characterized by a statistically significant (95% confidence level) negative trend (Fig. 3b). Following the mean 500 hPa anomaly patterns for the highest and the lowest factor 1 scores (Fig. S1a,b), high precipitation in the above area relates to high cyclonic activity over Italy (negative height anomalies), while low precipitation is connected to high anticyclonic activity over central Europe (e.g. Xoplaki et al. 2000, Bartzokas et al. 2003b). Factor 2 corresponds to eastern Thrace and western Asia Minor (Fig. 3a). High

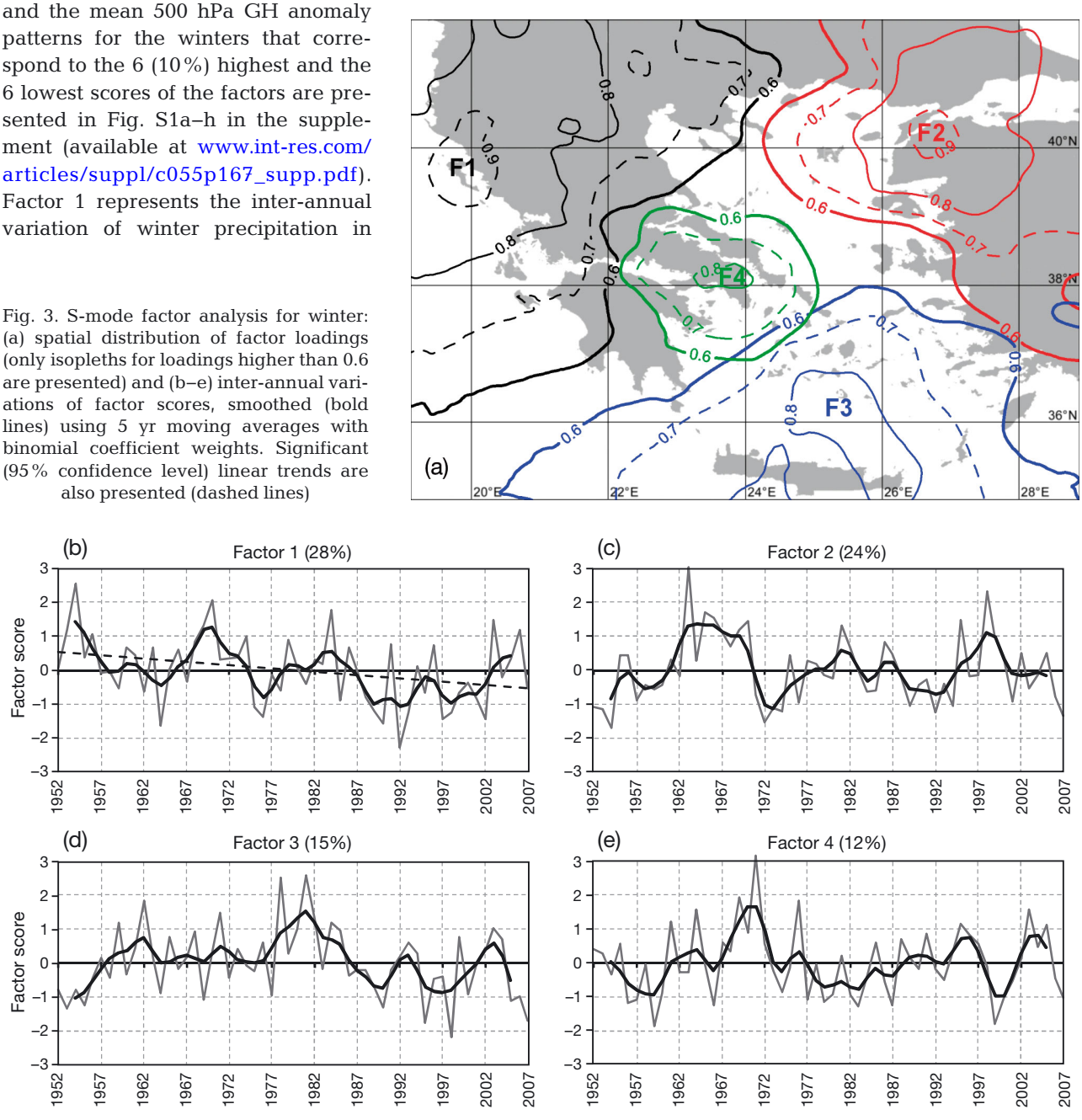

Fig. 3. S-mode factor analysis for winter: (a) spatial distribution of factor loadings (only isopleths for loadings higher than 0.6 are presented) and (b–e) inter-annual variations of factor scores, smoothed (bold lines) using 5 yr moving averages with binomial coefficient weights. Significant (95% confidence level) linear trends are also presented (dashed lines)

precipitation over this area is associated with high cyclonic activity over central Europe (Fig. S1c). These synoptic conditions promote a southwesterly flow over the southern Balkans. This flow passes over the Aegean Sea and contributes to high precipitation over western Asia Minor and eastern Thrace, as the presence of large aqueous bodies (e.g Aegean Sea) enhances evaporation and increases the humidity of the overlying air. In contrast, low precipitation over the same region can be attributed to high blocking activity over northern Europe, which is responsible for a dry catabatic northeasterly flow over the area of factor 2 (Fig. S1d). Factor 3 corresponds to the area of the south Aegean Sea and Crete (Fig. 3a). High cyclonic (anticyclonic) activity over Italy and the central Mediterranean is responsible for high (low) precipitation over the area of factor 3 (Fig. S1e,f). The main differences between the circulation characteristics affecting precipitation in the areas of factors 1 and 3 is that in the case of low precipitation, the positive anomaly center in factor 3 is displaced southwards relative to that of factor 1. Finally, factor 4 describes precipitation variability over the area of the southeastern Greek peninsula including Athens (Fig. 3a). High precipitation over this area is connected to low GH anomalies over the western (central) Mediterranean basin and high anomalies over central (northern) Europe (Fig. S1g). It is well documented that precipitation in Athens is favored by the presence of a depression in the central Mediterranean and an anticyclone over the northern Balkans. The combination between these systems frequently promotes a southeasterly flow over Athens, which is humid because of the passage of air masses over the Aegean Sea. Although precipitation in Athens in general can be linked to various circulation patterns associated with different surface wind directions, an easterly wind component over southeastern Greece may be responsible for the local enrichment of the air masses with water vapor over the Aegean Sea, contributing to high near-surface humidity levels and extreme precipitation events over the Athens area (e.g. Houssos et al. 2008, Michailidou et al. 2009).

For spring, the spatial distribution of mean precipitation is shown in Fig. 2b. It is generally similar to winter, because for middle and early spring (especially for March, which is the rainiest of the spring months), precipitation is a result of typical winter Mediterranean depression presence. The amounts are generally lower than those of winter. This is attributed to the fact that during spring the above depression activity gradually weakens because of the northward displacement of the jet stream and the increasing static stability over the sea which gradually becomes cooler relative to the overlying air (see e.g. Lolis 2007). Similarly to winter, the application of FA for spring leads to 4 factors accounting for 79% of the total variance. The spatial distribution of loadings (Fig. 4a) generally resembles that of winter. A statistically significant positive trend was found for factor 1 (western Asia Minor), which was also documented by Türkeş et al. (2009). Significant negative trends were found for factors 2 (northwest Greece to southern Albania) and 3 (south Aegean Sea; Fig. 4 b–e). The negative trend for northwestern Greece (factor 1) was also found for winter. The mean 500 hPa GH anomaly patterns for the highest and the lowest factor scores are presented in Fig. S2a–h in the supplement. High spring precipitation in western Asia Minor (factor 1) is favored by high cyclonic activity over the northern Balkans (negative GH anomalies), associated with a humid southwesterly flow passing over the Aegean Sea, while low precipitation is associated with anticyclonic activity over almost the whole European area, with the height anomaly maximum located around the south coasts of Asia Minor, close to the area of factor 1 (Fig. S2a,b). For the area of northwestern Greece (factor 2), the low and high GH anomaly centers are both located over the Gulf of Genoa, highlighting that the effect of the typical winter depressions on precipitation of the west windward areas of the southern Balkans is also dominant in spring (Fig. S2c,d). High spring precipitation over the southern Aegean Sea and Crete (factor 3) is generally attributed to frequent passages of Saharan depressions over this area (Trigo et al. 1999). These depressions are formed over the Atlas Mountains, and their formation is favored by the predominance of anticyclonic activity over northern Europe and cyclonic activity (cut-off lows) over the Gibraltar region (see e.g. Prezerakos et al. 1990). These circulation characteristics are generally in agreement with the locations of maxima and minima in the mean GH anomaly pattern for the highest factor 3 scores (Fig. S2e). In contrast, low precipitation over the south Aegean Sea is connected to positive GH anomalies over the whole area under study, especially over central Europe (Fig. S2f). Finally, precipitation over the Athens region (factor 4) is strongly affected by frequent upper air troughs over the Adriatic and the Ionian Seas usually accompanied by depressions centered over the Ionian Sea and humid southeasterly surface flows over the Aegean Sea (Fig. S2g).

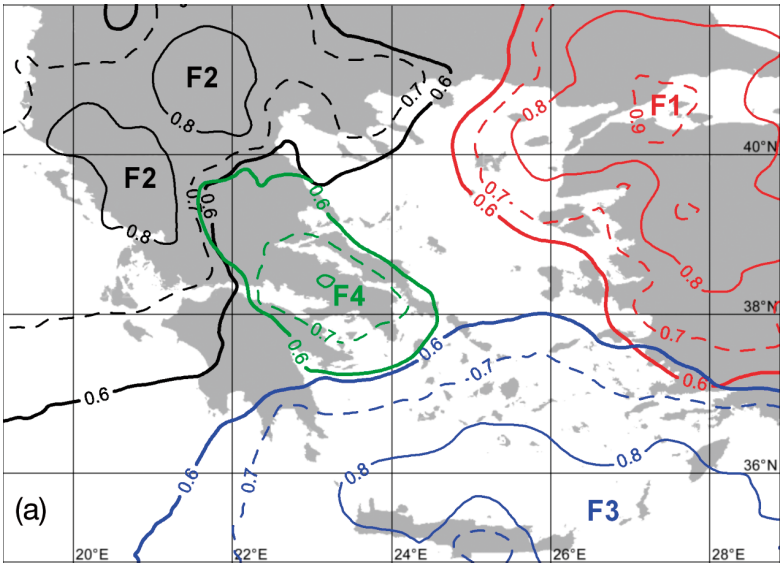

Fig. 4. S-mode factor analysis for spring: as in Fig. 3, but for spring

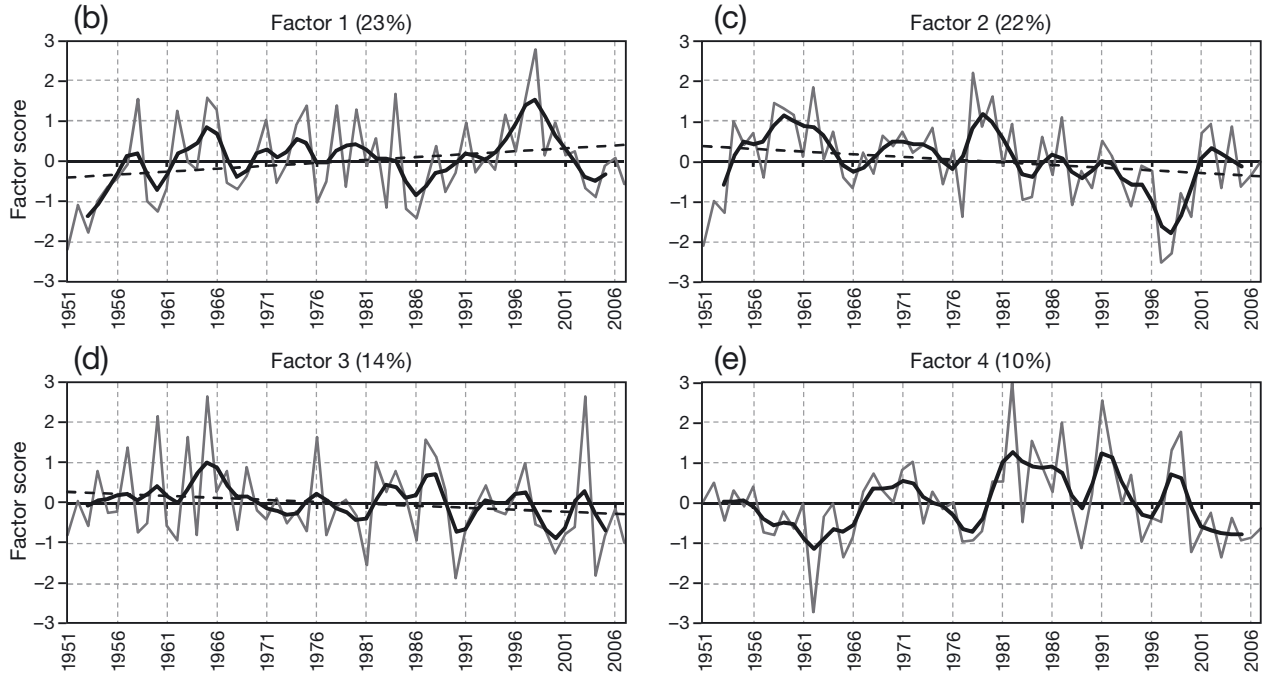

For autumn, the spatial distribution of the long-term mean precipitation is shown in Fig. 2c. The main difference between the patterns of autumn and winter is that while during winter the maxima of northwestern Greece and the western Asia Minor coasts are almost of the same magnitude, in autumn the maximum of northwestern Greece is of higher magnitude. This is due to the fact that after the summer dryness, the first autumn Mediterranean depressions move from west to east, affecting mainly the western windward areas, and then they move northeastwards towards the Black Sea, and thus not affecting the eastern Aegean Sea and the coasts of western Asia Minor as much (Lolis et al. 2008). The application of FA results in 5 factors (compared with 4 for winter and spring) accounting for 75% of the total variance. The isopleths of factor loadings and the inter-annual variations of factor scores are presented in Fig. 5, while the mean GH anomaly patterns for the highest and the lowest scores are shown in Fig. S3 in the supplement. The spatial distribution of high loadings is generally different to those of the other 2 seasons. Factor 1 corresponds to the area of eastern Thrace and northwestern Asia Minor and

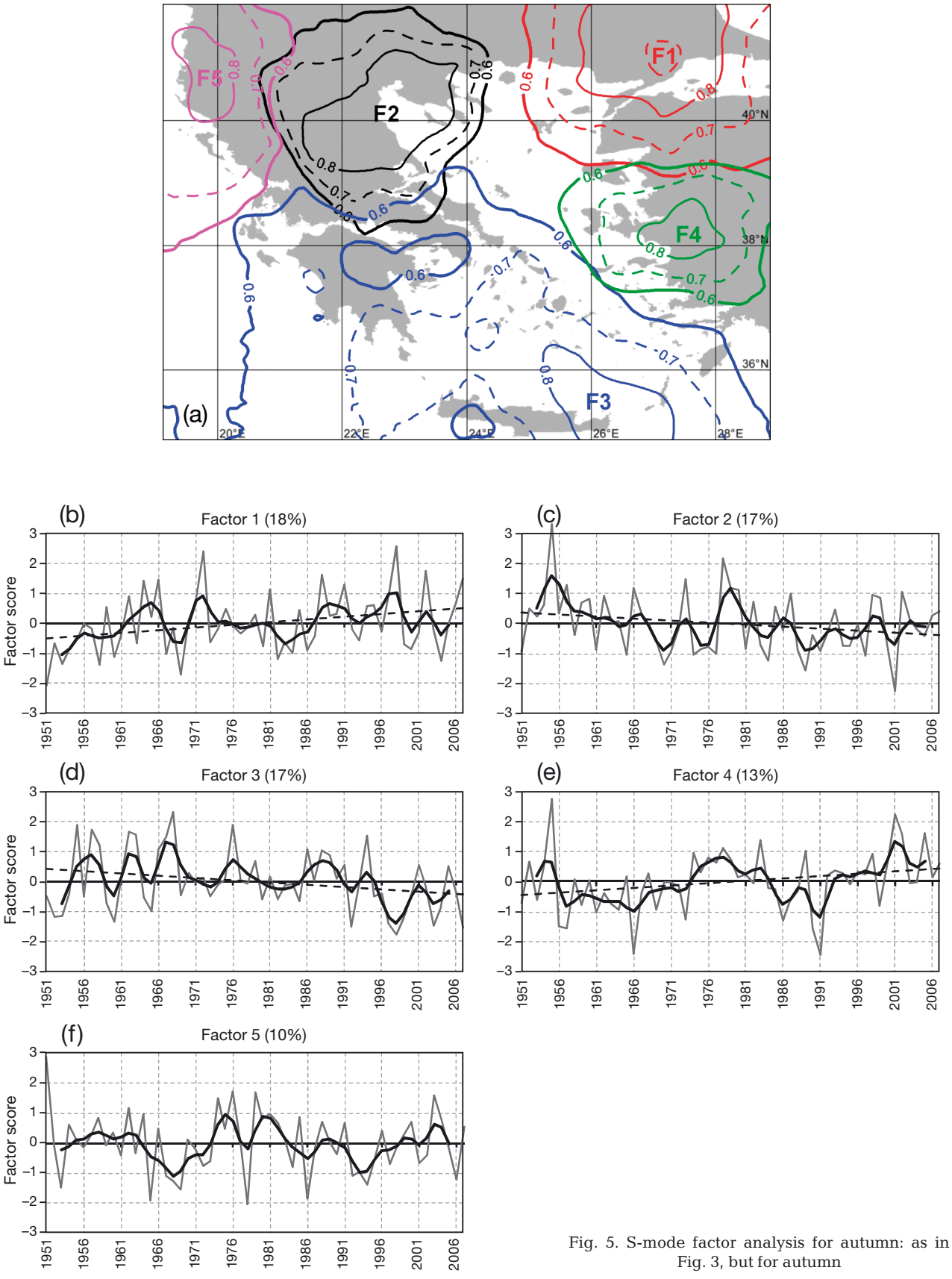

Fig. 5. S-mode factor analysis for autumn: as in Fig. 3, but for autumn

is characterized by a positive precipitation trend (Fig. 5b). High precipitation in this area is connected to high cyclonic activity over eastern Europe favoring a humid southwesterly flow passing over the Aegean Sea, while low precipitation is connected to high anticyclonic activity over approximately the same area favoring the advection of cold and dry air masses from the Siberian plateau (Fig. S3a,b). The northeastern Greek peninsula (factor 2) is characterized by a negative precipitation trend (Fig. 5c). The synoptic conditions characterized by the presence of a depression over the central Mediterranean south of Sicily and anticyclonic circulation over the northern Balkans lead to a high convergence over the area of factor 2 and the advection of humid air masses from the Aegean Sea via a southeasterly flow, which is responsible for high precipitation (Fig. S3c) (Houssos et al. 2008). In contrast, high cyclonic activity over eastern Europe is responsible for a northwesterly flow over the Balkans suppressing precipitation in the eastern Greek peninsula (Fig. S3d). Factor 3 corresponds to the area of the south Aegean Sea and Crete (Fig. 5a). This area is characterized by a precipitation reduction during the period under study (Fig. 5d). High precipitation in this area is favored by the frequent presence of depressions over the central Mediterranean and the persistence of anticyclonic activity over Russia, while low precipitation is associated with enhanced cyclonic activity over eastern Europe allowing the advection of warm and dry air masses from north Africa over the south Aegean Sea (Fig. S3e,f). Factor 4 corresponds to the central part of western Asia Minor and is characterized by a positive precipitation trend (Fig. 5e). High precipitation over the above area is favored by the presence of a cyclonic disturbance over the southern Balkans causing a humid southwesterly flow passing over the Aegean Sea, while low precipitation is associated with frequent or stationary low pressure systems over northwest Africa which, combined with an anticyclonic ridge over the northern Balkans, are responsible for a dry easterly flow over the area of factor 4 (Fig. S3g,h). Positive trends in autumn precipitation over western Asia Minor and eastern Thrace (factors 1 and 4) were also found by Türkeş et al. (2009). Finally, factor 5 corresponds to northwestern Greece, southern Albania, and the northern Ionian Sea. Precipitation in this area is generally favored by a warm and humid southwesterly anabatic flow associated with the presence of a large-scale cyclonic disturbance over western Europe and the western Mediterranean, while the persistence of intense anticyclones over central Europe is responsible for cold and dry catabatic flow over the same area, associated with sunny and dry weather (Fig. S3i,j).

In order to examine the possible connection between the factors and the known global-scale teleconnections over the North Atlantic Ocean and Eurasia, the correlation coefficients between the factor scores and the corresponding indices obtained from the CPC database (www.cpc.ncep.noaa.gov) were calculated (Table 1). The teleconnections are: the NAO, the East Atlantic Pattern (EA), the East Atlantic/Western Russia pattern (EA/WR), the Scandinavia pattern (SCA), and the Polar/Eurasia pattern (POL) (Barnston & Livezey 1987). NAO is mainly connected to precipitation in the western areas of Greece and Asia Minor (negative coefficients for these areas), but the coefficients are not statistically significant, except for the case of factor 2 for winter (western Asia Minor – east Thrace). Specifically, a high NAO index is associated with low precipitation (negative coefficient) in this area, as the frequent northeasterly flows prevailing during a positive NAO phase are dry and catabatic there. I found no statistically significant relation between EA and precipitation, while EA/WR is connected (negative statistically significant coefficients) to winter and autumn precipitation of northwestern Greece and southern Albania (winter – factor 1, autumn – factor 5). This

Table 1. Correlation coefficients between North Atlantic Oscillation (NAO), the East Atlantic Pattern (EA), the East Atlantic/Western Russia pattern (EA/WR), the Scandinavia pattern (SCA), and the Polar/Eurasia pattern (POL) indices and the factor scores time series. Significant (95% confidence level) coefficients are in **bold**

	Winter				Spring				Autumn				
	F1	F2	F3	F4	F1	F2	F3	F4	F1	F2	F3	F4	F5
NAO	−0.20	**−0.32**	−0.06	−0.08	−0.18	0.15	0.09	0.25	−0.24	0.00	−0.04	−0.24	−0.07
EA	−0.25	−0.06	−0.17	−0.22	−0.12	−0.24	−0.20	−0.13	−0.22	−0.12	−0.17	0.09	0.02
EA/WR	**−0.47**	−0.20	−0.14	0.02	−0.05	0.23	−0.09	0.09	−0.01	0.03	0.11	−0.18	**−0.34**
SCA	**0.41**	−0.07	−0.06	0.13	0.06	**0.35**	0.20	0.12	−0.15	−0.02	−0.07	0.06	0.09
POL	−0.10	0.15	0.21	0.19	0.15	−0.09	0.08	0.10	−0.15	−0.22	**0.47**	−0.04	−0.02

connection is attributed to the predominance of frequent southwesterly anabatic flows during years characterized by a low EA/WR index, as a low EA/WR index implies higher than normal cyclonic activity over the east Atlantic and higher than normal anticyclonic activity over western Russia. The SCA index is significantly correlated (positive coefficients) with winter and spring precipitation over northwestern Greece and southern Albania (factor 1 – winter, factor 2 – spring), as a high SCA index is associated with enhanced cyclonic activity in the central Mediterranean, accompanied by frequent southwesterly anabatic flows over these areas. Finally, the POL index is significantly correlated (positive coefficient) with autumn precipitation of southern Greece (autumn – factor 3), as a high POL index is associated with an enhanced anticyclonic activity over central Europe, being responsible for the advection of cool air masses over the Aegean Sea. In autumn, these air masses become unstable over the warm surface of the Aegean Sea, favoring precipitation over the southern Aegean Sea and Crete.

3.2. Intra-annual variability

The application of T-Mode FA on the mean 5 d precipitation values resulted in 3 factors accounting for 91% of the total variance. The spatial patterns of the scores show the main modes of precipitation spatial distribution in the southern Balkans, and the loadings time series show the intra-annual variations of their predominance. The spatial distributions of loadings and the intra-annual variations of scores are presented in Figs. 6–8.

Factor 1 (38% of the total variance) describes the 'cold period' type of precipitation spatial distribution, as the loadings exceed 0.7 (the 0.7 threshold corresponds to about 50% of the spatial variance) from mid-November to mid-March (Fig. 6a). The spatial distribution of scores presents maxima in northwestern Greece, southwestern Asia Minor coasts, and western Crete and minima over the south Aegean Sea and the eastern Greek peninsula (Fig. 6b). This spatial distribution is in agreement with the west to east movement of the typical cold period Mediterranean depressions, which generally promote southwesterly flow and high precipitation in the west windward areas during their passage over the southern Balkans. During this period of the year, atmospheric instability and relative vorticity over the central Mediterranean Sea are high, confirming the frequent passage of these depressions and their influence on precipitation of the western windward areas of the Balkan Peninsula (Lolis et al. 2008, 2012). The warm sea surface and the associated high upward sensible and latent heat fluxes and the high baroclinicity along the coasts of the northern Mediterranean Sea are the main factors leading to the formation and the intensification of these depressions (e.g. Trigo et al. 2002, Lolis et al. 2004).

Factor 2 (35% of the total variance) corresponds to the 'warm period' pattern of precipitation, as the

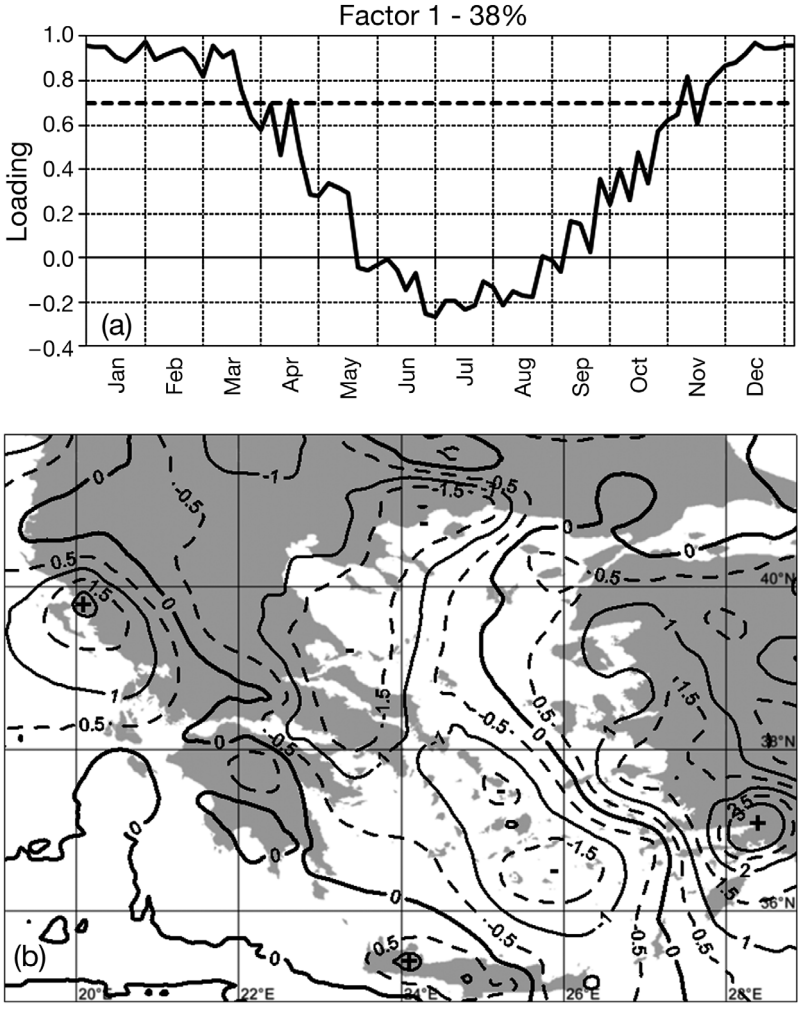

Fig. 6. T-mode factor analysis: (a) intra-annual variation of loadings (0.70 dashed line indicates the 50% variance threshold) and (b) spatial distribution of scores for factor 1

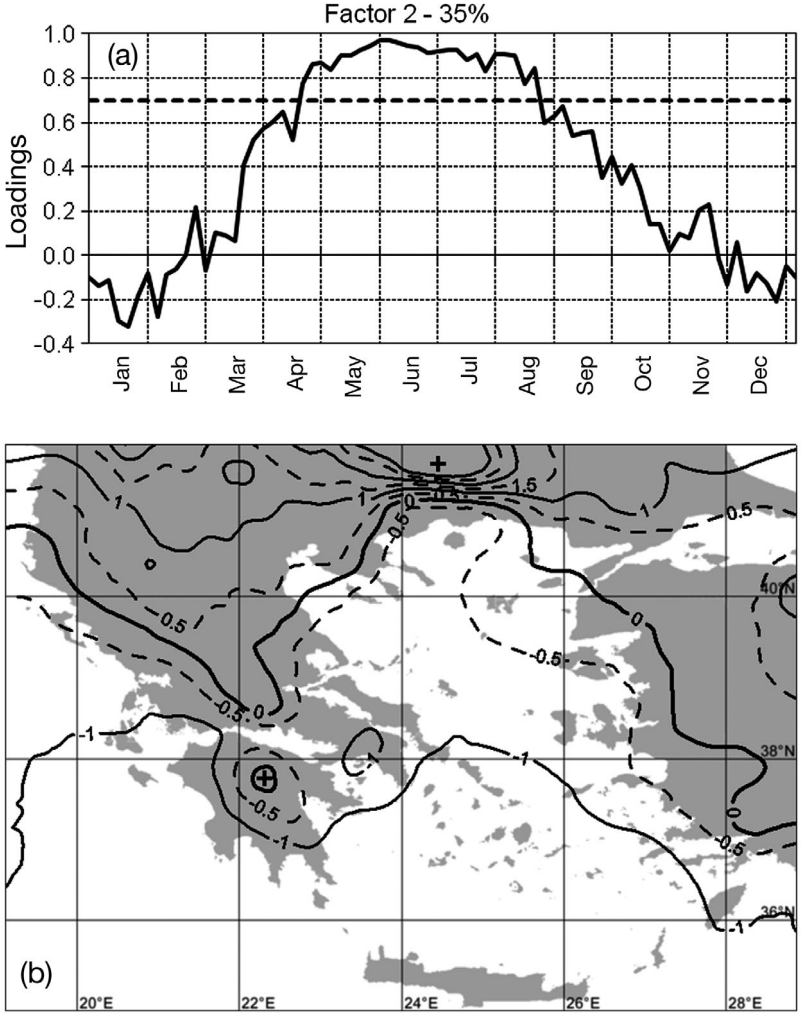

Fig. 7. T-mode factor analysis: as in Fig. 6, but for factor 2

loadings are highest from the middle of April to the end of August (Fig. 7a). During this period of the year, the spatial distribution of precipitation is characterized by maxima over the northern and continental areas and low values over the southern sea areas (Fig. 7b). This pattern is in agreement with the fact that during the warm period of the year, precipitation is mainly a result of upper air disturbances and high static instability associated with cold air masses in the middle troposphere. These conditions lead to high precipitation and thunderstorm activity mainly over the northern and continental areas because of the significant land warming and not over the sea where the surface atmospheric layers are very stable because of the very cool sea surface (relative to the air above it; Chronis 2012). For the warm period of the year, the high static stability and the associated anticyclonic activity over the Mediterranean sea surface on one hand and the high static instability and the enhanced cyclonic activity over the continental areas north of the Mediterranean Sea on the other hand are clearly shown in the works of Lolis et al. (2008, 2012) for relative vorticity and static stability. The spatial distribution of the above parameters over the Mediterranean region provides more evidence for the interpretation of the warm period precipitation pattern over the southern Balkans. This precipitation pattern is also in agreement with the summer pattern found by Hatzianastassiou et al. (2008) over the same region using GPCP precipitation data.

Factor 3 (18% of the total variance) describes the 'autumn' pattern of precipitation, which prevails from the end of August to the end of October (Fig. 8a). This pattern is characterized by a maximum over the northern Ionian Sea and a minimum over western Asia Minor (Fig. 8b). As already mentioned above, this spatial distribution is associated with the fact that the first depressions formed after summer dryness generally move northeastwards towards the Black Sea, affecting mainly the northwestern parts of the area under study. This autumn pattern is similar to the autumn pattern found by Bartzokas et al. (2003a) with the use of 10 d rain gauge precipitation data over Greece. According to both Bartzokas et al. (2003a) and the present study, the 3 main climatic patterns of precipitation in Greece are the cold period, the warm period, and the autumn patterns, while the location of the maxima and minima are in about the same positions. The latter supports the validity of the APHRODITE precipitation data set for the area of the southern Balkans.

4. CONCLUSIONS

The inter- and intra-annual variability of precipitation in the southern Balkans was examined, applying S-Mode and T-Mode FA to APHRODITE 0.25° × 0.25° precipitation data. The following conclusions can be made:

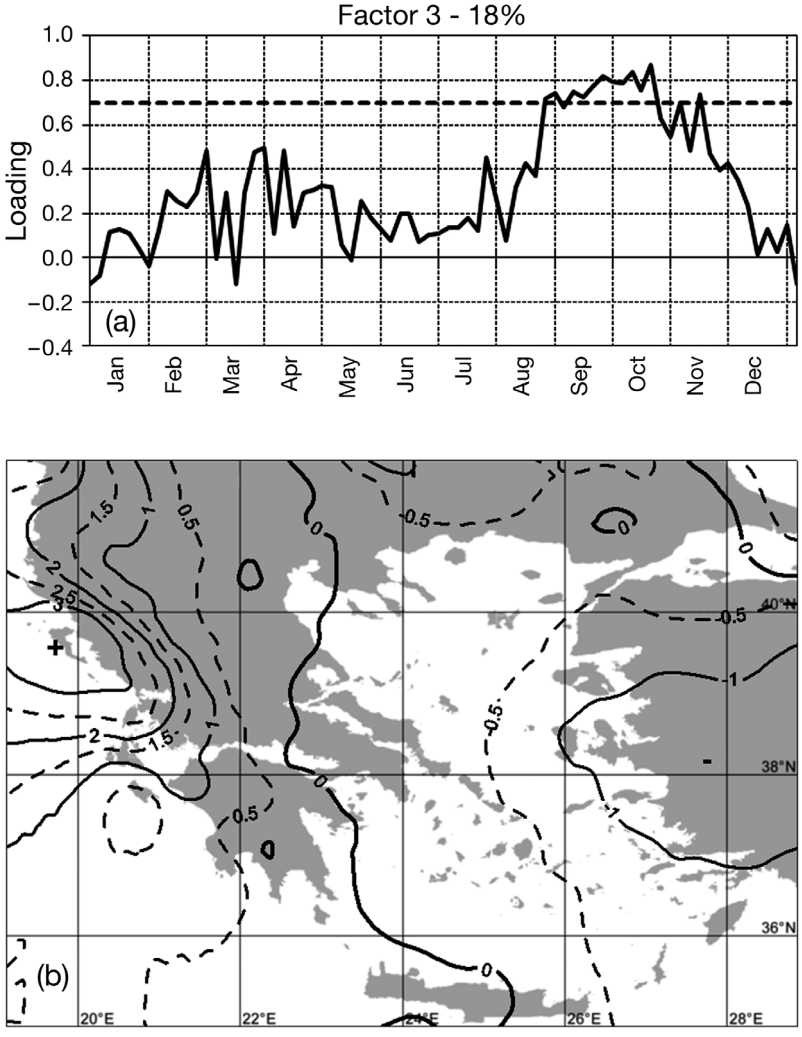

Fig. 8. T-mode factor analysis (FA): as in Fig. 6, but for factor 3

(1) Winter and spring precipitation in the southern Balkans is generally affected by the typical cold season Mediterranean depressions and is controlled by the same centers of action.

(2) Autumn precipitation presents some different characteristics relative to winter and spring, and this is mainly due to the different depression trajectories that prevail during this season.

(3) Winter and spring precipitation in northwestern Greece and southern Albania, and spring and autumn precipitation in the southern Aegean Sea and Crete, present a statistically significant decrease during the period 1951–2007, associated with a corresponding increase of anticyclonic activity in the central Mediterranean. The above negative precipitation trends are generally in agreement with the future scenarios of climate models, and can result in a significant reduction of the available water resources in these areas. Thus, they need to be taken into account by governments and policy makers dealing with water management, agriculture, and other sectors of social and economic activity related to weather and climate.

(4) Some connections were found between precipitation in the southern Balkans and the known global-scale teleconnections over the North Atlantic Ocean and Eurasia. Specifically, the indices of the NAO, EA/WR, SCA, and POL were found to be significantly correlated to precipitation in the area under study.

(5) Three main types of spatial distribution of precipitation were found: the cold period, the warm period, and the autumn type. The differences among the 3 types are connected to the differences in the origin of precipitation (frontal or thermal) and the prevailing depression trajectories.

(6) Taking into account the findings of other recent studies on spatial and temporal precipitation variability in the southern Balkans, my findings show that the APHRODITE precipitation data set satisfactorily describes the main characteristics of precipitation in the area under study.

LITERATURE CITED

Alpert P, Tsidulko M, Krichak S, Stein U (1996) A multi-stage evolution of an ALPEX cyclone. Tellus 48A:209–220

Barnston MP, Livezey RE (1987) Classification, seasonality and persistence of low frequency atmospheric circulation patterns. Mon Weather Rev 115:1083–1126

Bartzokas A, Metaxas DA (1993) Covariability and climatic changes of the lower-troposphere temperatures over the Northern Hemisphere. Nuovo Cimento C 16:359–373

Bartzokas A, Lolis CJ, Metaxas DA (2003a) A study on the intra-annual variation and the spatial distribution of precipitation amount and duration over Greece on a 10 day basis. Int J Climatol 23:207–222

Bartzokas A, Lolis CJ, Metaxas DA (2003b) The 850 hPa relative vorticity centres of action for winter precipitation in the Greek area. Int J Climatol 23:813–828

Chronis TG (2012) Preliminary lightning observations over Greece. J Geophys Res 117:D03113, doi:10.1029/2011JD017063

Chronis T, Raitsos DE, Kassis D, Sarantopoulos A (2011) The summer North Atlantic Oscillation influence on the eastern Mediterranean. J Clim 24:5584–5596

Davis RE, Hayden BP, Gay DA, Phillips WL, Jones GV (1997) The North Atlantic subtropical anticyclone. J Clim 10: 728–744

Fotiadi AK, Metaxas DA, Bartzokas A (1999) A statistical study of precipitation in NW Greece. Int J Climatol 19: 1221–1232

García-Serrano J, Rodríguez-Fonseca B, Bladé I, Zurita-Gotor P, de la Cámara A (2011) Rotational atmospheric circulation during North Atlantic-European winter: the influence of ENSO. Clim Dyn 37:1727–1743

Hatzianastassiou N, Katsoulis BD, Pnevmatikos J, Antakis V (2008) Spatial and temporal variation of precipitation in Greece and surrounding regions based on Global Precipitation Climatology Project data. J Clim 21:1349–1370

Houssos EE, Lolis CJ, Bartzokas A (2008) Atmospheric circulation patterns associated with extreme precipitation amounts in Greece. Adv Geosci 17:5–11

Hurrel JW, van Loon H (1997) Decadal variations in climate associated with the North Atlantic Oscillation. Clim Change 36:301–326

Javanmard S, Yatagai A, Nodzu MI, Bodagh Jamali J, Kawamoto H (2010) Comparing high-resolution gridded precipitation data with satellite rainfall estimates of TRMM 3B42 over Iran. Adv Geosci 25:119–125

Jolliffe IT (1986) Principal component analysis. Springer-Verlag, New York, NY

Kalnay E, Kanamitsu M, Kistler R, Collins W and others (1996) The NCEP/NCAR 40-year reanalysis project. Bull Am Meteorol Soc 77:437–471

Kambezidis HD, Larissi IK, Nastos PT, Paliatsos AG (2010) Spatial variability and trends of the rain intensity over Greece. Adv Geosci 26:65–69

Kistler R, Kalnay E, Collins W, Saha S and others (2001) The NCEP/NCAR 50-year reanalysis: monthly means CD-ROM and documentation. Bull Am Meteorol Soc 82: 247–267

Kotini-Zabaka S (1983) Contribution to the study of the climate of Greece. Normal weather per month. Publication No. 8. Research Centre of Climatology of the Academy of Athens (in Greek)

Lolis CJ (2007) Climatic features of atmospheric stability in the Mediterranean region (1948-2006): spatial modes, inter-monthly and inter-annual variability. Meteorol Appl 14:361–379

Lolis CJ, Bartzokas A, Katsoulis BD (2004) Relation between sensible and latent heat fluxes in the Mediterranean and precipitation in the Greek area during winter. Int J Climatol 24:1803–1816

Lolis CJ, Metaxas DA, Bartzokas A (2008) On the intra-annual variability of atmospheric circulation in the Mediterranean region. Int J Climatol 28:1339–1355

Lolis CJ, Bartzokas A, Lagouvardos K, Metaxas DA (2012) Intra-annual variation of atmospheric static stability in the Mediterranean region: a 60-year climatology. Theor Appl Climatol 110:245–261

Maheras P, Flocas HA, Patrikas I, Anagnostopoulou C (2001) A 40 year objective climatology of surface cyclones in the Mediterranean region: spatial and temporal distribution. Int J Climatol 21:109–130

Manly BFJ (1986) Multivariate statistical methods: a primer. Chapman & Hall, London

Metaxas DA, Bartzokas A (1994) Pressure covariability over the Atlantic, Europe and N. Africa. Application: centers of action for temperature, winter precipitation and summer winds in Athens, Greece. Theor Appl Climatol 49: 9–18

Metaxas DA, Philandras CM, Nastos PT, Repapis CC (1999) Variability of precipitation pattern in Greece during the year. Fresenius Environ Bull 8:1–6

Michailidou C, Maheras P, Arseni-Papadimititriou A, Kolyva-Machera F, Anagnostopoulou C (2009) A study of weather types at Athens and Thessaloniki and their relationship to circulation types for the cold-wet period. I. two-step cluster analysis. Theor Appl Climatol 97: 163–177

Nastos PT (2011) Trends and variability of precipitation within the Mediterranean region, based on Global Precipitation Climatology Project (GPCP) and ground based datasets. In: Lambrakis N, Stournaras G, Katsanou K (eds) Advances in the research of aquatic environment, Vol 1. Environmental Earth Sciences Series. Springer, Berlin, p 67–74

Overland JE, Preisendorfer RW (1982) A significant test for principal components applied to cyclone climatology. Mon Weather Rev 110:1–4

Philandras CM, Nastos PT, Kapsomenakis J, Douvis KC, Tselioudis G, Zerefos CS (2011) Long term precipitation trends and variability within the Mediterranean region. Nat Hazards Earth Syst Sci 11:3235–3250

Prezerakos NG, Michaelides SC, Vlassi AS (1990) Atmospheric conditions associated with the initiation of northwest African depressions. Int J Climatol 10:711–729

Richman MB (1986) Rotation of principal components. J Climatol 6:293–335

Tatli H, Türkeş M (2011) Empirical orthogonal function analysis of the Palmer drought indices. Agric For Meteorol 151:981–991

Thorncroft CD, Flocas HA (1997) A case study of Saharan cyclogenesis. Mon Weather Rev 125:1147–1165

Trigo IF (2006) Climatology and interannual variability of storm-tracks in the Euro-Atlantic sector: a comparison between ERA-40 and NCEP/NCAR reanalyses. Clim Dyn 26:127–143

Trigo IF, Davies TD, Bigg GR (1999) Objective climatology of cyclones in the Mediterranean region. J Clim 12: 1685–1696

Trigo IF, Bigg GR, Davies TD (2002) Climatology of cyclogenesis mechanisms in the Mediterranean. Mon Weather Rev 130:549–569

Türkeş M, Koç T, Saris F (2009) Spatiotemporal variability of precipitation total series over Turkey. Int J Climatol 29: 1056–1074

Unal YS, Deniz A, Toros H, Incecik S (2012) Temporal and spatial patterns of precipitation variability for annual, wet, and dry seasons in Turkey. Int J Climatol 32: 392–405

Xoplaki E, Luterbacher J, Burkard R, Patrikas I, Maheras P (2000) Connection between the large-scale 500 hPa geopotential height fields and precipitation over Greece during wintertime. Clim Res 14:129–146

Yatagai A, Xie P, Alpert P (2008) Development of a daily gridded precipitation data set for the Middle East. Adv Geosci 12:165–170

Yatagai A, Arakawa O, Kamiguchi K, Kawamoto H, Nodzu MI, Hamada A (2009) A 44-year daily gridded precipitation dataset for Asia based on a dense network of rain gauges. SOLA 5:137–140

Yatagai A, Kamiguchi K, Arakawa O, Hamada A, Yasutomi N, Kitoh A (2012) APHRODITE: constructing a long-term daily gridded precipitation dataset for Asia based on a dense network of rain gauges. Bull Am Meteorol Soc 93: 1401–1415

Editorial responsibility: Oliver Frauenfeld, College Station, Texas, USA

Submitted: April 4, 2012; Accepted: August 9, 2012
Proofs received from author(s): November 30, 2012